Reaction channel contributions to the proton + ^{208}Pb optical potential at 40 MeV

R. S. Mackintosh [*]
School of Physical Sciences, The Open University, Milton Keynes MK7 6AA, United Kingdom

N. Keeley [†]
National Centre for Nuclear Research, ul. Andrzeja Sołtana 7, 05-400 Otwock, Poland

(Received 25 August 2022; accepted 10 November 2022; published 28 November 2022)

Background: Reaction channel coupling substantially modifies the real and imaginary nucleon-nucleus interactions for nuclei of $Z = 20$ or less in ways that cannot be represented as uniform renormalizations of folding model potentials. For such nuclei coupling to inelastic channels also contributes. This raises the question of the effect of these couplings for heavier target nuclei.
Purpose: To establish and characterize the contribution to the proton-nucleus interaction generated by coupling to neutron pickup (outgoing deuteron) channels for 40 MeV protons on the heavy closed shell nucleus ^{208}Pb. To identify and evaluate the consequent dynamical non-locality.
Methods: Coupled reaction channel (CRC) calculations provide the elastic channel S-matrix S_{lj} due to the included processes. Inversion of S_{lj} will produce the local potential that would yield, in a single channel calculation, the elastic scattering observables from the CRC calculation. Subtracting the bare potential of the CRC calculations gives a local and l-independent representation of the dynamical polarization potential (DPP). From the DPPs due to various combinations of channel couplings, the influence of dynamically generated nonlocality can be identified.
Results: Coupling to deuteron channels generates a repulsive component for the real potential and an absorptive component for the imaginary term. The radial shapes of both terms were modified in ways that could not be represented by uniform renormalization; the rms radius of the real part was substantially altered. Evidence of the dynamical nonlocality of the DPP due to pickup is provided by the nonadditivity of contributions of different couplings and other effects. For the doubly closed shell ^{208}Pb coupling to low-lying (nongiant) collective states has a very small effect on elastic scattering, making a negligible contribution compared with pickup, and was not included.
Conclusions: The DPPs established here strongly challenge the notion that folding models, in particular local density models, provide a satisfactory description of elastic scattering of protons from heavy nuclei. Coupling to neutron pickup channels induces dynamical nonlocality in the proton optical model potential with implications for direct reactions.

DOI: 10.1103/PhysRevC.106.054611

I. INTRODUCTION

It has long been established that collective and reaction channel processes play an essential role in understanding the elastic scattering of both nucleons and composite nuclei, see, e.g., Ref. [1]. These processes have an important influence on elastic scattering observables. This influence cannot be represented in theories based on local density models; couplings to these channels induce contributions that cannot be represented by uniform renormalization of potentials based on such models. In previous works we have shown that for protons scattering from nuclei as heavy as ^{48}Ca [2] coupling to neutron pickup channels (outgoing deuterons) can be particularly important. In the present work we extend these studies to the heavy target ^{208}Pb which gives access to a large number of strongly populated pickup channels having a wider range of angular momentum transfers than in previous work. The contribution of neutron pickup to the proton-nucleus interaction is thus expected to be particularly strong for the elastic scattering of protons on ^{208}Pb. The contribution of pickup, for 40 MeV protons, is the subject of the extensive study in this paper. It will turn out that for 40 MeV protons scattering from ^{208}Pb, the contribution of inelastic coupling to low-lying collective states is relatively small and is not included.

The formal contribution to the nucleon optical model potential (OMP) of such processes as inelastic or reaction channel coupling is both nonlocal and l-dependent [1,3,4]. The nonlocality referred to here is distinct from the nonlocality due to exchange processes and will be referred to as dynamical nonlocality in what follows, see Ref. [5]. However, the contribution to elastic scattering of various particular inelastic or reaction processes can be represented as a local and l-independent addition to the phenomenological potential. This addition is the local representation

[*] raymond.mackintosh@open.ac.uk
[†] nicholas.keeley@ncbj.gov.pl

of the dynamical polarization potential (DPP). As described in Sec. II, this is found by determining the local and l-independent potential that exactly reproduces the S-matrix S_{lj} from the coupled channel (CC) calculations using $S_{lj} \rightarrow V(r) + \boldsymbol{l}\cdot\boldsymbol{s}\, V_{\rm SO}(r)$ inversion [6–9]. This establishes the connection with elastic scattering experimental data and standard local phenomenology. See Refs. [2,5,10–13] for applications of this 'CC-inversion' procedure to much lighter target nuclei than in the present case. For nucleon scattering from the lighter nuclei the balance between inelastic processes and transfer contributions turns out to be substantially different to what we find for the heavy closed shell nucleus ^{208}Pb. For DPPs for the scattering of mass-3 nuclei, see Refs. [14,15].

In this paper, 'coupled channels' includes coupled reaction channels (CRC) as well as coupling to inelastic channels, etc., unless specifically noted; also, references to 'local' potentials can usually be taken to mean 'local and l-independent'.

II. DETERMINATION OF THE DPPS FOR PROTONS ON ^{208}Pb

The DPPs are determined following the CC-inversion procedure outlined in the Introduction. The present ^{208}Pb case presents a more stringent test of CC inversion than the previously published applications involving lighter nuclei, up to ^{48}Ca. The inversion method has its limits, and the present case is challenging. There is no problem in determining the DPP due to (p, d) coupling to a single state of ^{207}Pb, but that due to the simultaneous coupling to all six states listed below is not possible; each state separately generates a formal DPP that is nonlocal and l-dependent. We have found that determining, by inversion, the local and l-independent representation of the combined effect of six such terms leads to divergence of the CC-inversion procedure.

A natural question is, why not invert the S_{lj} from the coupling to each of the six states individually and add the resulting local potentials? Recall that the formal DPPs for each state are nonlocal and l-dependent; the local equivalent of the sum of such contributions is not the sum of the local equivalents of each term. The results presented below demonstrate this nonadditivity of the local DPPs. Many important and interesting cases of DPPs arising from coupling to multiple states have been studied, Refs. [2,5,10–13] and earlier work cited therein. Establishing the DPP due to the simultaneous pickup of the six states of ^{208}Pb proves challenging.

In cases of coupling to various states it would be natural to determine an optimum bare potential for each particular case, and this would be important if one was attempting to extract spectroscopic factors, for example. However, it is of interest to record the nonadditivity of the local DPPs, and this would be obscured if each DPP were calculated with a different bare potential, so we employ a single bare potential for each pickup state. Fortunately, calculated DPPs do not depend strongly on the bare potential, the original potential to which the coupling is added, as long as it is 'reasonable', see Ref. [16], and this is exploited in the present work.

III. REACTION CHANNELS FROM ^{208}Pb

For the ^{208}Pb target we studied the contributions of (p, d) coupling to six states of ^{207}Pb. To these states we have assigned labels L1, L2, etc., which will simplify the identification of cases involving multiple coupled states. The states of ^{207}Pb are:

L1: 0.0 MeV $\frac{1}{2}^-$, $l = 1$;

L2: 0.57 MeV $\frac{5}{2}^-$, $l = 3$;

L3: 0.90 MeV $\frac{3}{2}^-$, $l = 1$;

L4: 1.633 MeV $\frac{13}{2}^+$, $l = 6$;

L5: 2.34 MeV $\frac{7}{2}^-$, $l = 3$;

L6: 3.413 MeV $\frac{9}{2}^-$, $l = 5$.

A case will be designated L4L6 when there is coupling to both the L4 and L6 levels. Coupling to levels L2, L4, and L6 will be designated L2L4L6, etc. Thus the L4 case is that in which there is an amplitude for (p, d) pickup from the $\frac{13}{2}^+$ neutron orbital of ^{208}Pb. The L4L6 case is that in which there are amplitudes for (p, d) pickup of both $\frac{13}{2}^+$ and $\frac{9}{2}^-$ neutrons of ^{208}Pb.

It is important that the DPP for coupling L4L6 is not the sum of the DPPs for case L4 and for case L6. This is indicative of dynamical nonlocality, as we shall discuss. Coupling L2L4L6 is the same as L6L4L2; the CC code does not distinguish the order of the couplings. Three of the coupled states have $j = l + \frac{1}{2}$ and three have $j = l - \frac{1}{2}$ and it will turn out that the spin-orbit terms of the DPP will be correlated with this difference, particularly for the L1 and L3 cases.

The L6, $\frac{9}{2}^-$, state has the largest effect on the elastic scattering differential cross section beyond about 90 degrees whereas the L4, $\frac{13}{2}^+$, state has the largest effect forward of 90 degrees.

In the present calculations the target is one of the best examples of a doubly magic nucleus and we have taken the pickup spectroscopic factors and neutron binding potentials from the (p, d) study of Matoba *et al.* [17]. Unlike the cases for lighter target nuclei, Refs. [2,5,10–13], for protons on the doubly closed shell ^{208}Pb the contribution of inelastic scattering, at least to lower lying collective states, turns out to be very small and inelastic coupling is not included in the present work.

A. Details of the pickup coupling

The CRC calculations were performed with the code FRESCO [18] and included both the full complex remnant term and nonorthogonality correction. The choice of bare optical potential for the entrance channel is discussed in the following section. For the exit channel(s) we used the global deuteron optical potential parameters of Daehnick *et al.* [19]. The $\langle d \mid n + p\rangle$ overlap was calculated using the Reid soft-core potential [20] and included the small D-state component. The $\langle ^{208}\text{Pb} \mid ^{207}\text{Pb} + n\rangle$ overlaps were calculated using the parameters given in Matoba *et al.* [17]. These were obtained from a distorted wave Born approximation (DWBA) analysis of ^{208}Pb(p, d) data at 65 MeV, and when used as input to the CRC calculations described here give a satisfactory

description of the 41 MeV ^{208}Pb$(p, d)^{207}$Pb data of Smith *et al.* [21], provided the entrance channel optical model parameters are readjusted in each case to fit the elastic scattering data. This proviso has an important bearing on the dynamical nonlocality demonstrated in this work.

B. The bare potential

Attempts to define a bare potential by fitting the elastic scattering data when all states, L1 to L6, were coupled simultaneously, were found to be impossible; the fitting procedure for 40 MeV protons on ^{208}Pb is not as straightforward as it was for 30.3 MeV protons on ^{40}Ca, Ref. [13]. Coupling to as many as three pickup states simultaneously poses no problems, either to fitting the elastic scattering data or to inverting the resultant S_{lj}. Coupling more states becomes problematical; the cumulative effect of the couplings is so strong now that it was difficult to arrive at as good a fit to the elastic scattering as desired, i.e., comparable to typical optical model fits. Moreover, it did not prove possible to obtain a reliable inversion of the corresponding S_{lj}.

The study of the nonlocality of the DPPs, and other properties, requires a fixed bare potential for each inversion, L1 to L6. For this reason we exploit the finding of Ref. [16], as well as trial calculations, to the effect that calculated DPPs are not strongly dependent on the bare potential. Accordingly, the bare potential, which will be applied in all cases, was determined by fitting the elastic scattering data, differential cross section and analyzing power, for case L4, i.e., for coupling to the $\frac{13}{2}^+$ at 1.633 MeV in the middle of the range of excitation energies. Case L4 and case L6 were also those with the strongest effect on the calculated elastic scattering differential cross section.

The bare potential was based on the CH89 global proton parameters [22], to which an imaginary spin-orbit (SO) term was added, of the same geometry as the real part. Seven of the resulting 15 standard Woods-Saxon parameters were searched on V, a_v, W, $W_{\rm D}$, $r_{\rm D}$, $a_{\rm D}$, and $W_{\rm SO}$, using the notation of Ref. [1]. The remaining eight parameters were kept fixed at CH89 values. The fit to the elastic scattering data with the L4 coupling on (solid lines) is presented in Fig. 1; the data are those of Blumberg *et al.* [23]. The dashed lines represent the results when the L4 coupling is switched off. It will be seen that L4 coupling halves the differential cross section around 150 degrees.

Various combinations of reaction channel couplings have been studied. For example, from the DPPs for cases L4, L6, and L4L6 the nonadditivity of DPPs will be evident, and the subject of interpretation.

IV. EVALUATING THE DPPs

The local equivalent DPPs for coupling to specified coupled channels are determined as follows. The four components of the bare potential are subtracted from the corresponding components of the potential determined by inverting S_{lj} for the elastic channel when calculated with the specified coupled channels. The four components include the real and imaginary spin-orbit terms, essential for fitting S_{lj} arising from the coupling. Characteristic properties of the DPPs for various combinations of the possible couplings are presented in Table I in terms of the differences between corresponding properties of the inverted and bare potentials. The radial forms for the DPPs are presented in Sec. IV A.

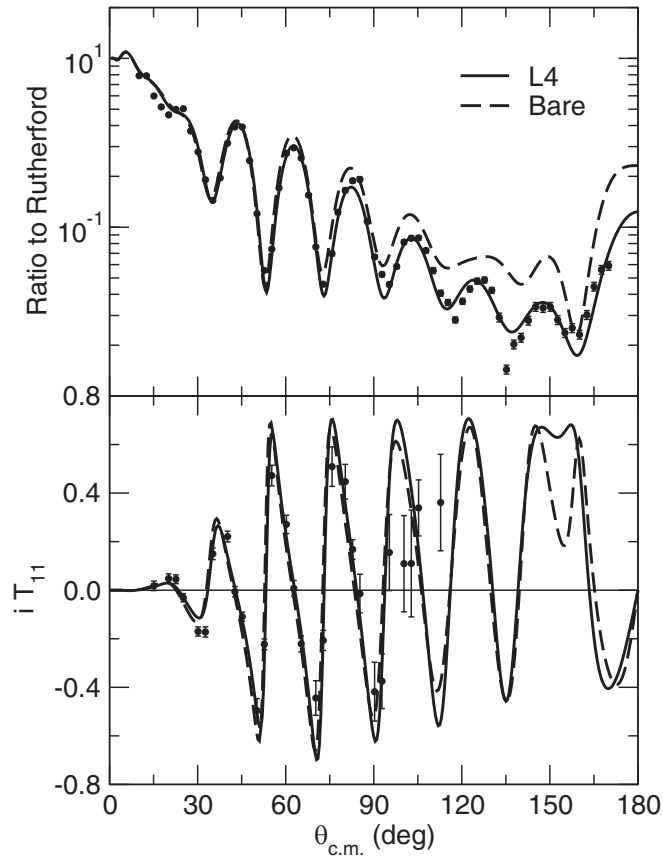

FIG. 1. For protons on ^{208}Pb at 40 MeV, the solid lines present the fit to the elastic scattering data when L4 coupling is included. The dashed lines are calculated with the same fitted bare potential but no coupling. The upper panel presents the differential cross section and the lower panel presents the analyzing power.

In Table I we employ the standard normalization of Ref. [1] for $J_{\rm R}$ and $J_{\rm IM}$, the volume integrals of the real and imaginary potentials. We also adhere to the standard sign convention, in which a positive sign represents attraction or absorption. Thus, a negative value for $\Delta J_{\rm R}$ represents an overall repulsive contribution to the real central potential from the particular coupling in question. However, the more natural sign convention is employed in the figures showing the potentials. Line 4 presents numerical sums of quantities in lines 1 and 2, and lines 7 and 13 similarly present sums of the indicated couplings. These lines will be significant in a discussion of dynamical nonlocality.

For each coupling, Table I also presents Δ(CS), the change in reaction cross section (CS) due to the coupling. The quantity R is the ratio of Δ(CS) to $\Delta J_{\rm IM}$, the change, due to coupling, in the volume integral of the imaginary central

TABLE I. For proton scattering from ^{208}Pb at 40 MeV, volume integrals ΔJ (in MeV fm^3) of the four components of the DPP induced by (p, d) pickup coupling, The coupled states for ^{208}Pb are given in Sec. III; the excitation energies of the states, in MeV, are all specified. The $\Delta R_{\rm rms}$ column gives the change in rms radius of the real central component (in fm). The final four columns present, respectively, the change in the total reaction cross section induced by the coupling, the integrated cross section to the specific coupled reaction channels, the ratio R and the ratio $R_{\rm CS}$, both defined in the text. Note that negative $\Delta J_{\rm R}$ corresponds to repulsion, as is usual for PU. The quantities Δ(CS) and State CS are given in mb. Line 4 presents numerical sums of the quantities in lines 1 and 2; lines 7 and 13 also present such sums.

L	Coupling	$\Delta J_{\rm R}$	$\Delta J_{\rm IM}$	$\Delta J_{\rm RSO}$	$\Delta J_{\rm IMSO}$	$\Delta R_{\rm rms}$	Δ(CS)	State CS	R	$R_{\rm CS}$
1	L4	−8.49	12.77	−0.212	0.0405	0.0196	28.2	3.431	2.21	8.22
2	L6	−5.85	11.618	0.1397	−0.540	0.0564	18.4	1.755	1.58	10.48
3	L4L6	−14.86	33.198	−0.3128	0.1307	0.1414	46.0	4.993	1.39	9.21
4	L4 + L6	−14.34	24.388	−0.0273	−0.4995	0.076	46.6	5.186	1.91	8.99
5	L2	−8.06	7.568	0.3318	−0.2107	0.0165	26.2	7.393	3.46	3.54
6	L2L4L6pot6	−34.52	69.728	0.3714	−3.3525	0.2422	67.9	11.731	0.97	5.79
7	L2+L4L6	−22.92	40.766	0.019	−0.080	0.1579	72.2	13.386	1.77	5.39
8	L5	−6.85	4.599	−0.383	0.0295	0.0018	20.3	5.692	4.41	3.57
9	L2L4L6pot5	−36.35	67.318	0.7639	−0.1363	0.2199	69.6	11.731	1.03	5.93
10	L1	−3.29	2.567	0.1117	−0.0040	0.0010	12.8	4.613	4.99	3.08
11	L3	−6.20	4.479	0.0261	0.00373	0.003	22.5	8.077	5.02	2.79
12	L1L3	−10.53	7.305	0.1656	−0.0339	0.0087	34.4	12.43	4.71	2.77
13	L1 + L3	−9.49	7.046	0.1378	−0.0003	0.0040	35.3	12.69	5.01	2.78
14	L4X	−15.91	19.00	−0.554	−0.0702	−0.0129	34.0	13.30	1.79	2.56

potential

$$R = \frac{\Delta(\mathrm{CS})}{\Delta J_{\rm IM}}. \tag{1}$$

R varies over a much smaller range than Δ(CS) or $\Delta J_{\rm IM}$ separately. We do not give SI units but the behavior of R is meaningful within a particular case.

Table I also presents the 'State CS' which is the total (p, d) cross section in mb for the relevant pickup state or states as specified in the text. It gives a measure of the coupling. The state CS is not necessarily equal to the change in reaction cross section Δ(CS) and the relationship between the two can vary widely, Refs. [2,14,15], depending on the particular case. In cases where inelastic coupling is included together with reaction channel coupling [2,14,15], the relation between Δ(CS) and State CS is quite different for pickup and inelastic collective coupling. Various relationships have emerged for different cases and to facilitate comparisons, we present values of $R_{\rm CS}$ defined as the ratio of Δ(CS) to State CS. In all cases in the present work, the increase in the reaction cross section exceeds the cross section to the pickup state or states. It seems that the pickup channels behave as a doorway to other processes [2,15].

Regarding the comparison of the DPPs for different couplings, it is important to recall that all calculations for each target nucleus were carried out with a fixed bare potential: the potential that was determined as explained in Sec. II.

The L2L4L6 case presented a challenge to S_{lj} to V inversion and lines 6 and 9 correspond to two independent inversions. Not all calculated quantities are exactly the same, but the key point is that the comparison with line 7 does clearly reveal the nonadditivity. In particular $\Delta J_{\rm R}$ and $\Delta J_{\rm IM}$ in lines 6 and 9 are very close when compared with the values of these quantities in line 7, demonstrating the robustness of the nonadditivity that signals nonlocality, as discussed below.

By contrast, the coupling to two more weakly coupled states, L1 and L3, led to S_{lj} that were very easy to invert, leading to DPPs that were correspondingly smaller in magnitude. The general properties of the inverted potentials were the same as for the more strongly coupled states, including the non-additivity property to be discussed below.

A. Radial form of the DPPs

The L4 and bare potentials corresponding to Fig. 1 are presented in Fig. 2. Repulsion is evident between 4 fm and 8 fm with some attraction elsewhere. The net repulsive effect is reflected in the negative $\Delta J_{\rm R}$ in Table I and the attraction, just visible beyond 8 fm, accounts for the positive $\Delta R_{\rm rms}$.

The L6 coupling is also substantial and the DPP is presented in Fig. 3. The real central component has a significant repulsive region around 6 fm and some attraction around 8.5 fm. This is similar to the effects due to L4 coupling. While the imaginary central term is dominated by absorption around 7 fm, there are emissive regions around 4 fm and 10 fm. The oscillatory structure that appears in all components is a more or less universal property of DPPs and can be related to a degree of l dependence of the formal DPP, see for example Ref. [4]. Such structure is a feature when l dependent potentials are represented by l-independent potentials having the same S matrix, Ref. [24].

The L2 and L5 DPPs, presented in Fig. 4 also exhibit repulsion in the real central component but the absorption appears to be less overall. The challenge is to relate the difference to the different L transfers, Q values, and spectroscopic factors. The larger magnitudes of both $\Delta J_{\rm R}$ and $\Delta J_{\rm IM}$ for the L2 case are clearly represented in the forms of the L2 and L5 curves for the central potential terms and the opposite signs for the real spin-orbit terms.

The DPPs for the weaker L1 and L3 states are presented in Fig. 5. The magnitude of the L3 form is greater than that

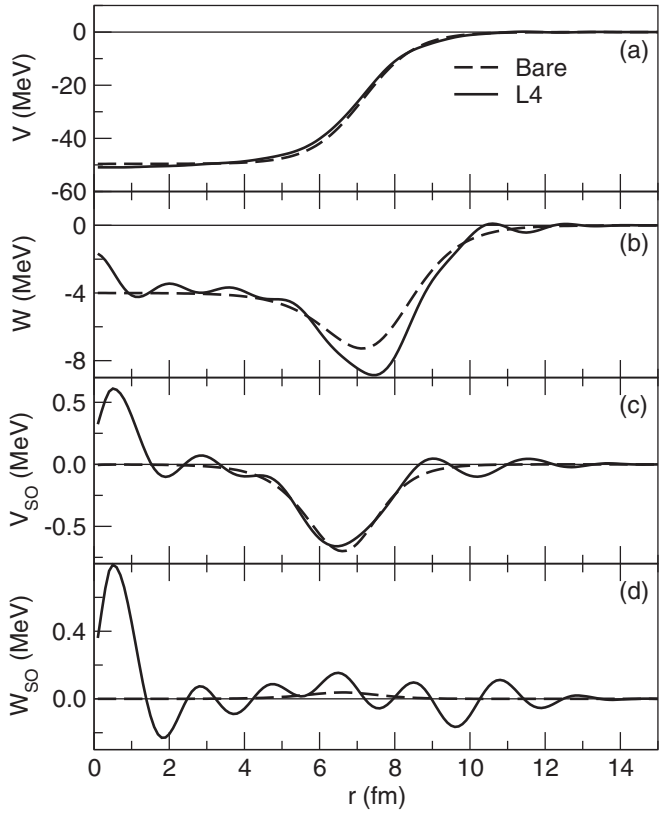

FIG. 2. For protons on ^{208}Pb at 40 MeV, the dashed lines present the bare potential and the solid lines present the inverted potential for L4 coupling corresponding to the solid line in Fig. 1. (a) presents the real central potentials, (b) presents the imaginary central potentials, (c) presents the real spin-orbit potentials, and (d) presents the imaginary spin-orbit potentials.

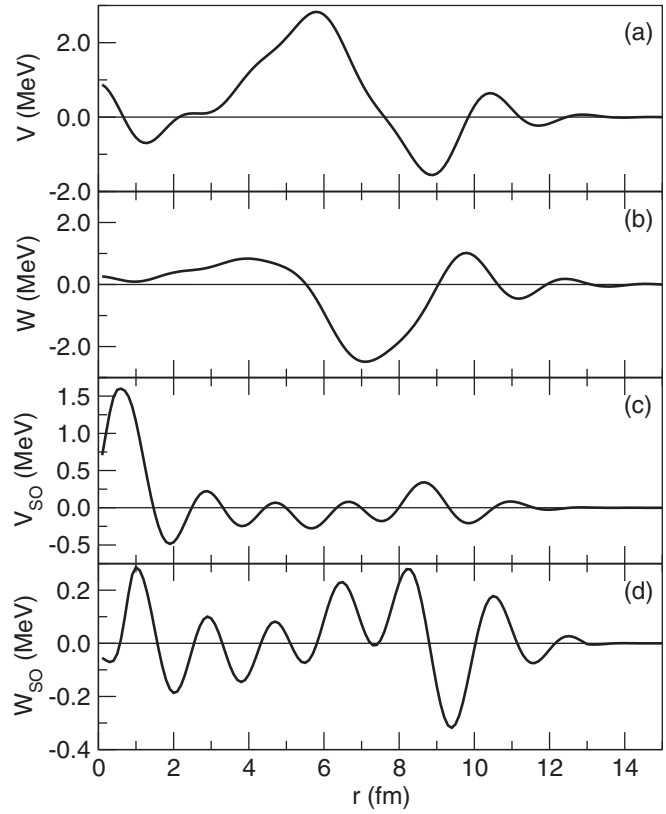

FIG. 3. For protons on ^{208}Pb at 40 MeV, the solid lines present the DPP generated by L6 coupling. (a) presents the real central potential, (b) presents the imaginary central potential, (c) presents the real spin-orbit potential, and (d) presents the imaginary spin-orbit potential.

of L1, in line with the greater magnitudes of ΔJ_{R} and ΔJ_{IM}. The apparent weakness of the coupling in terms of volume integrals relates to the fact that the DPPs have maximum magnitude at a smaller radius than the DPPs of the L2 and L5 cases. Both coupled states L1 and L3 are states with $l = 1$, lower than the other states. The coupled states L2 and L5 of Fig. 4, both have $l = 3$, and a comparison with Fig. 5 suggests a relationship between the radius of the DPP and the l of the coupled state: smaller l leads to DPPs mostly at lower radii. In Fig. 5, the significant difference in radial forms of the real and imaginary spin-orbit terms must relate to the fact that state L1 has $j = l - \frac{1}{2}$ and state L3 has $j = l + \frac{1}{2}$. It is harder to discern such a relationship in Fig. 4 for coupling to the $l = 3$ states since the DPPs are small in magnitude and are somewhat oscillatory; a possible artifact for DPPs of small magnitude, but also possibly due to l dependence.

B. Systematic correlates of l transfer or j transfer

The l of the transferred neutron appears to be correlated with quantities R and R_{CS}. This would be of particular interest if these trends persisted at other energies and for other cases. For l transfer of 5 or 6 (cases L4 and L6), the change in the reaction cross section is an order of magnitude greater than the cross section of the neutron transfer with R_{CS} about 10. For l transfer of 1 (cases L1 and L3), the change in the reaction cross section is about three times the cross section of the neutron transfer, with R_{CS} about 3. It seems that good practice would be to record values of the State CS in studies such as this.

Other systematic effects can be seen in the radial form of the DPPs, which extend to a greater radius for larger values of the l transfer. Comparing the spin-orbit DPPs for cases L1 and L3 (both $l = 1$) we note that both the real and imaginary parts have opposite signs for $j = l + \frac{1}{2}$ and $j = l - \frac{1}{2}$.

C. Evidence for dynamical nonlocality

Table I contains evidence for dynamical nonlocality. Lines 3 and 4 compare the various derived quantities for the L4L6 case with the sums of all the corresponding quantities for cases L4 and L6 separately. Likewise, lines 6 and 7 compare the calculated quantities for case L2L4L6 with the sums of the same quantities for cases L4L6 and L2; line 9 presents an alternative to line 6, as discussed below. It will be noted that for either alternative the DPPs for the mutual coupling cases are stronger that the sum of the DPPs for coupling to the L2 state and L4L6 states separately.

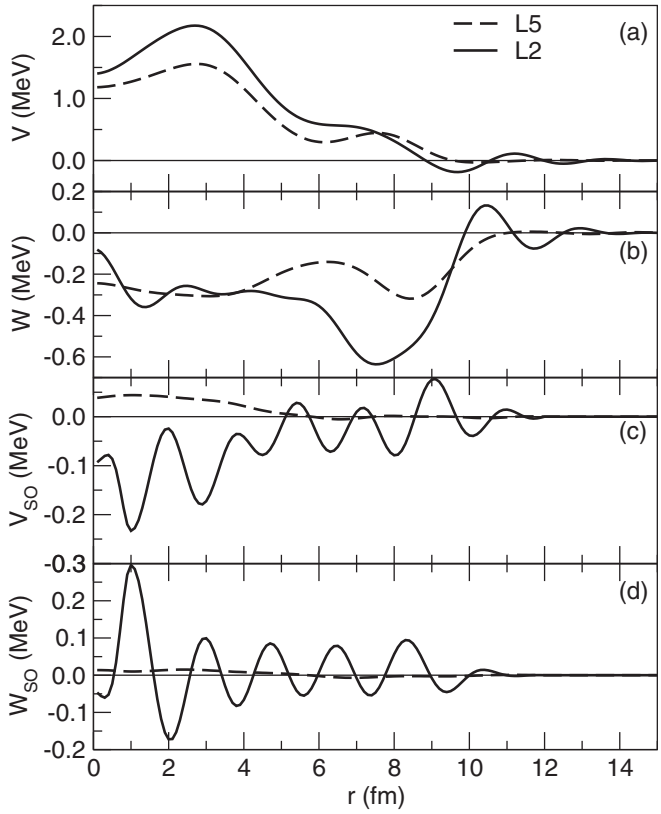

FIG. 4. For protons on ^{208}Pb at 40 MeV, the solid lines present the DPPs arising from L2 coupling and the dashed lines arising from L5 coupling. (a) presents the real central potentials, (b) presents the imaginary central potentials, (c) presents the real spin-orbit potentials, and (d) presents the imaginary spin-orbit potentials.

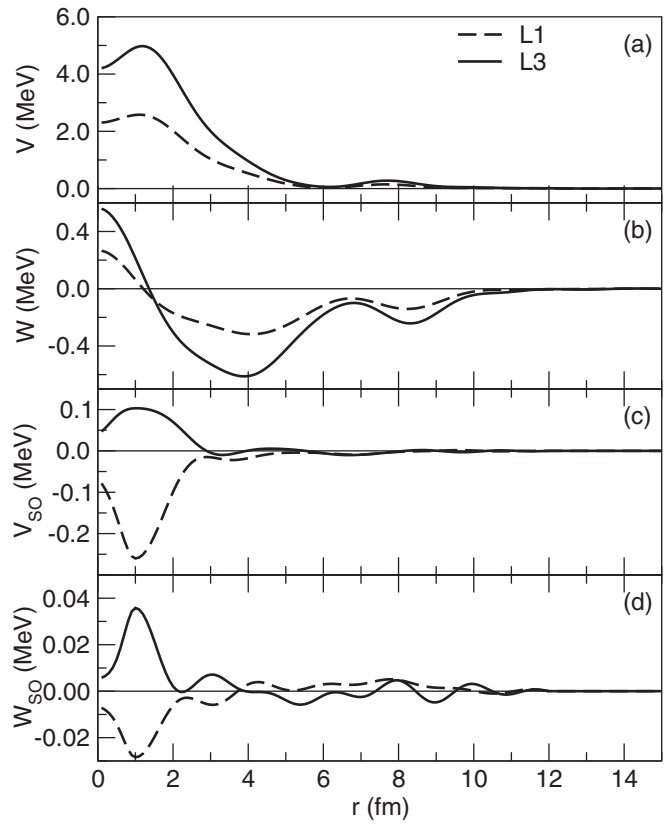

FIG. 5. For protons on ^{208}Pb at 40 MeV, the solid lines present the DPPs arising from L3 coupling and the dashed lines arising from L1 coupling. (a) presents the real central potentials, (b) presents the imaginary central potentials, (c) presents the real spin-orbit potentials, and (d) presents the imaginary spin-orbit potentials.

Table I thus contains evidence of dynamical nonlocality such that channels that are not mutually coupled nevertheless influence each other, see Ref. [5].

Behind this nonadditivity is the fact that the formal DPP for coupling to any particular state is nondiagonal in the r coordinate, i.e., nonlocal with form $V(r_1, r_2)$ [1,3,4]. Such nonlocal potentials, nondiagonal in r, were studied by Austern [25] in response to the phenomenological nonlocal potential of Ref. [26]. It is known that the local equivalents of such nonlocal potentials *do not add*; that is to say that the local equivalent of a sum of nonlocal potential terms is not the sum of the local equivalents of each term. 'Local equivalents' refers to local potentials that yield the same elastic scattering S matrix, S_{lj}, as the nonlocal potential. The consideration of the local equivalent provides a link to local phenomenology.

The nonadditivity is true for exchange non-locality, Ref. [26], as well as the dynamical nonlocality derived by Feshbach [3], see also Ref. [1]. The nondiagonal, and also l-dependent nature of the formal DPP is very apparent in the explicit calculations of Ref. [4]. In a calculation of the contribution, made by channel coupling, to a local and l-independent potential, the nonadditivity has the following consequence: contributions from two independent reaction or inelastic channels will not add to reproduce the contribution when both channels are active together.

The two cases above (i) (L4 + L6) compared to L4L6 and (ii) (L4L6 + L2) compared to L2L4L6, both exemplify the nonadditivity. The nonadditivity of the DPPs is immediately apparent in Fig. 6 which compares the L4L6 DPP with the sum of the L4 and L6 DPPs, and Fig. 7 which compares the L2L4L6 DPP with the sum of the L4L6 and L2 DPPs. Figure 8 compares the angular distributions for scattering with the (L4 + L6) and L4L6 potentials of Fig. 6. The difference is appreciable at backward angles; the dots in the figures represent the data for guidance.

We note here that the imaginary central DPP, particularly for the L4 and L6 cases, tends to have a relatively emissive region for $r \leqslant 4$ fm, This does not breach unitarity of course.

The nonadditivity for the weaker coupling states L1 and L3 is presented in Fig. 9 where the DPP for the L1L3 case is compared with the sum of the L1 and L3 DPPs. Apart from the imaginary spin-orbit term, the nonadditivity is most significant for $r < 2$ fm. The nonadditivity of the L1 and L3 DPPs is evident only for r less that about 4 fm and so is unlikely to be of importance for fitting data, yet Fig. 9 incidentally supports the consistency of the $S_{lj} \rightarrow V(r) + \boldsymbol{l} \cdot \boldsymbol{s}\ V_{\rm SO}(r)$ inversion. The agreement beyond about 4 fm is reassuring concerning the 'wavy' form of the DPP.

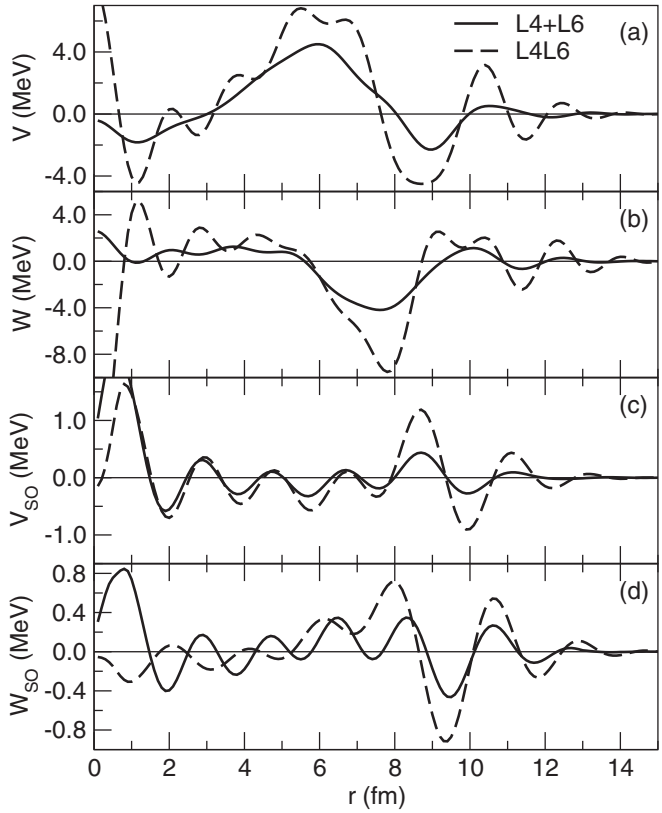

FIG. 6. For protons on ^{208}Pb at 40 MeV, the dashed lines present the DPP for case L4L6 and the solid lines present the sums of the DPPs for cases L4 and L6. (a) presents the real central potentials, (b) presents the imaginary central potentials, (c) presents the real spin-orbit potentials, and (d) presents the imaginary spin-orbit potentials.

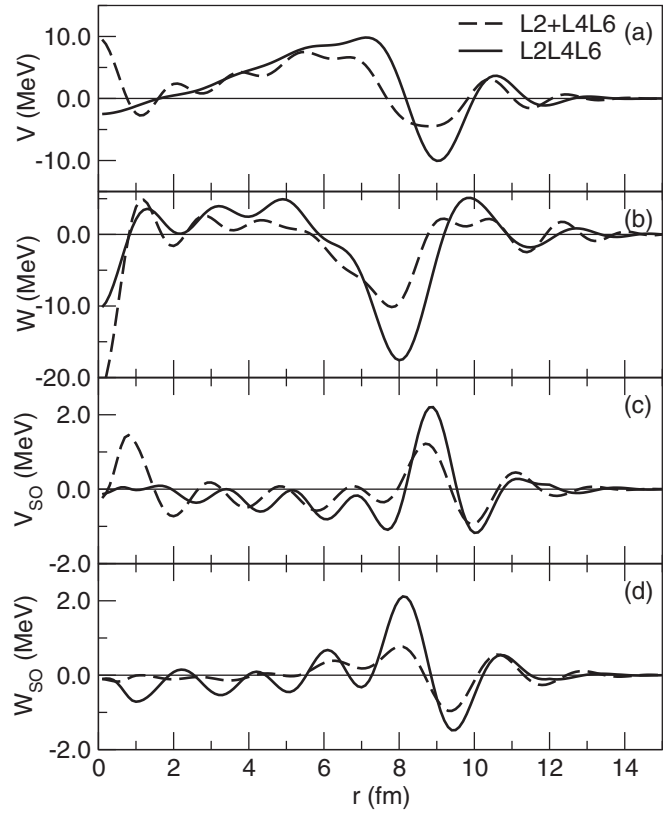

FIG. 7. For protons on ^{208}Pb at 40 MeV, the solid lines present the DPP for case L2L4L6 and the dashed lines present the sums of the DPPs for case L2 and case L4L6. (a) presents the real central potentials, (b) presents the imaginary central potentials, (c) presents the real spin-orbit potentials, and (d) presents the imaginary spin-orbit potentials.

The nonlocality of the DPPs that arises from channel coupling is of interest from two quite different standpoints. One is that local potentials are central to nuclear phenomenology: they are fitted to elastic scattering data and the object of global parameter sets, they are essential for obtaining nuclear structure information from direct reactions and they are the goal of folding model theories and, more generally, the practical derivation of nucleus-nucleus interactions. But the local potentials are nevertheless representations of nonlocal potentials and even when they yield the same elastic scattering, they will have different effects when applied in reaction calculations. The second standpoint is the general importance of nonlocality, seemingly of different kinds, in quantum physics.

D. Complete pickup contribution

Determining the total contribution of pickup coupling is nontrivial. Inverting the S matrix when only three states are coupled in a single calculation is nontrivial, as suggested by a comparison of lines 6 and 9. There are possible ways to get around this, but inverting S_{lj} for a calculation involving all of L1 to L6 simultaneously would be difficult.

We have estimated the full effect as follows: We have determined limits to $\Delta J_{\rm R}$ and $\Delta J_{\rm IM}$ for a complete calculation by postulating that the overall $-\Delta J_{\rm R}$ is greater than the sum of the $-\Delta J_{\rm R}$ values for lines 8, 9, and 12, in which the effects of couplings L1 to L6 are included. Likewise the overall change to $\Delta J_{\rm IM}$ would be greater than the sum of the $\Delta J_{\rm IM}$ values for lines 8, 9, and 12. We find the limits of the overall changes in volume integrals to be

$$-\Delta J_{\rm R} \geqslant 53.18 \ \ {\rm MeV} \ \ {\rm fm}^3, \tag{2}$$

$$\Delta J_{\rm IM} \geqslant 81.92 \ \ {\rm MeV} \ \ {\rm fm}^3 \tag{3}$$

of which the second in particular seems quite large. For 40 MeV protons on ^{208}Pb good Woods-Saxon fits were found [27] for which $J_{\rm IM} = 121.06\,{\rm MeV\ fm}^3$. Taken literally this would imply that about 70% of the absorption of protons scattering from ^{208}Pb at 40 MeV arises from neutron pickup. More realistically, we can affirm that our model implies that most of the absorption of 40 MeV protons on ^{208}Pb is due to pickup.

One line of investigation would be to study how the imaginary DPP depends upon the imaginary part of the deuteron optical model potential (OMP). What is clear is that pickup coupling, with standard CC formalism and a standard deuteron OMP, makes a very strong contribution to the proton-^{208}Pb interaction which is dynamically nonlocal and

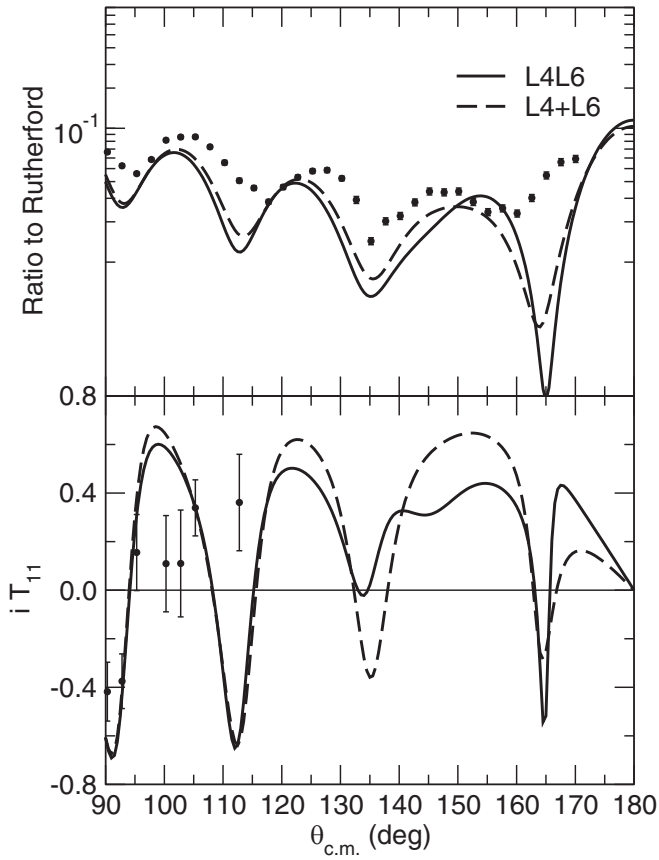

FIG. 8. For protons on ^{208}Pb at 40 MeV, the solid lines present differential cross section and analyzing power calculated with the L4L6 DPP added to the bare potential and the dashed lines present the same quantities calculated with the numerical sum of the L4 and L6 DPPs. The dots represent the experimental data. The upper panel presents the differential cross section and the lower panel presents the analyzing power.

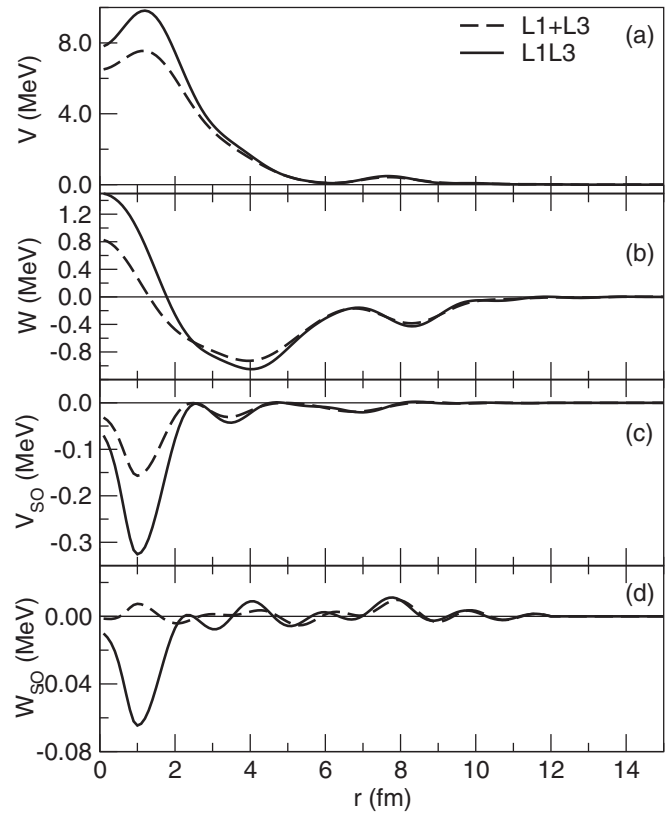

FIG. 9. For protons on ^{208}Pb at 40 MeV, the solid lines present the DPP for case L1L3 and the dashed lines present the sums of the DPPs for case L1 and case L3. (a) presents the real central potentials, (b) presents the imaginary central potentials, (c) presents the real spin-orbit potentials, and (d) presents the imaginary spin-orbit potentials.

cannot be represented as a renormalization of a folding model OMP.

The problem of determining the full effect of the pickup coupling, including the apparent effect of dynamical nonlocality, is illustrated in Fig. 10. Both the solid and dashed curves reflect contributions from pickup to all six states. The solid line simply represents the sum of the DPPs of each pickup channel alone. The dashed line presents a sum of terms such as L2L4L6 which represents the DPP when the L2, L4, and L6 states are all coupled, and other terms which together have a representation of all pickup states. This figure, and the others presented above all suggest that the real DPP is repulsive within the nucleus and the imaginary DPP is concentrated at about 8 fm, with some emissivity near 10 fm reflecting l-dependence.

E. Other evidence of dynamical nonlocality

There is evidence for dynamical non-locality which is not related to the potentials found by $S_{lj} \rightarrow V(r) + \boldsymbol{l} \cdot \boldsymbol{s}\ V_{\rm SO}(r)$ inversion. We refer to the State CS, the cross section to the particular coupled states as given in the State CS column of Table I. The values of the State CS also do not add; this is not related to inversion of S_{lj}. Compare the State CS values on lines 3 and 4 and also on lines 6 and 7. In both of these cases the State CS when both channels (L4 and L6 or L2 and L4L6) are coupled is less than the sums (4.993 c.f. 5.186 or 11.731 c.f. 13.386). The same relationship is found in lines 12 and 13 for the State CS values for cases L1 and L3.

The present cases are all such that ΔCS (the change in reaction cross section) is *much* greater than the corresponding State CS, see Refs. [2,15] for a discussion of this. In the present case, comparison of ΔCS values in lines 3 and 4 of Table I and also in lines 6 and 7 reveals that the increase in reaction CS when states are included together is somewhat less than the sum of ΔCS values when both sets of states are not included. This also seems to hold true for the much weaker L1 and L3 couplings, although the effect is very small.

Reference [5] demonstrated how the nonlocality generated by channel coupling modifies the DWBA (p, d) and (n, d) angular distributions for pickup reactions in which there is no channel coupling directly involving the specific transfer reactions. The nonlocality in the nucleon channel is due to inelastic couplings unrelated to the pickup reaction. There was a clear difference between the (p, d) and (n, d) angular distributions depending on whether the nucleon potential

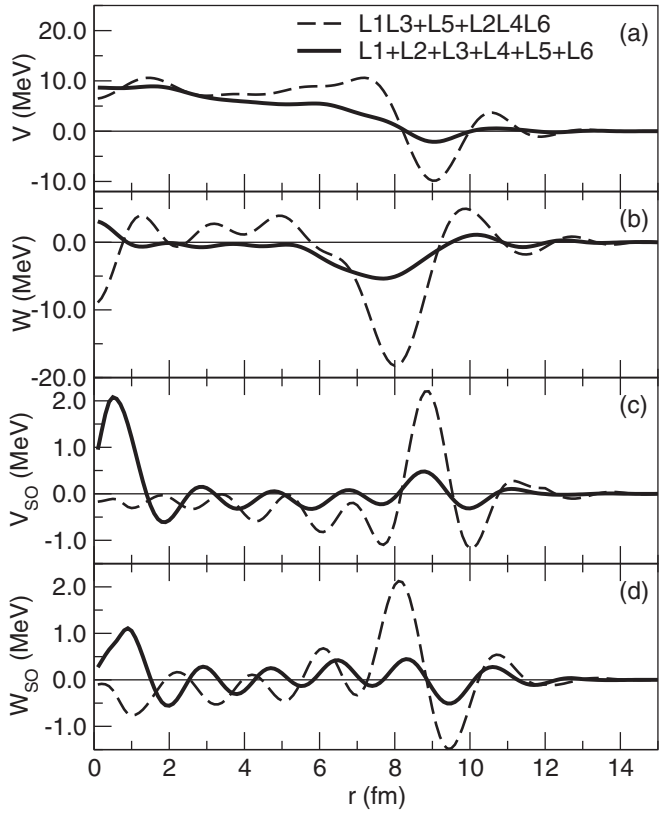

FIG. 10. For protons on ^{208}Pb at 40 MeV, the solid lines present the sum of the DPPs for all cases L1 to L6. The dashed lines present the DPP for the sum of the three cases, L1L3, L5, and L2L4L6. (a) presents the real central potentials, (b) presents the imaginary central potentials, (c) presents the real spin-orbit potentials, and (d) presents the imaginary spin-orbit potentials.

was dynamically nonlocal or the local S-matrix equivalent. In that case the nonlocality was generated by coupling to many collective states. The pickup angular distributions were very different, particularly at backward angles, for alternative proton potentials, local and nonlocal, that gave identical elastic scattering angular distributions.

Somewhat similarly, in Ref. [15] effects were found at backward angles for (^{3}H, ^{4}He) on ^{16}O for nonlocality generated by coupling of the ^{3}H to a collective channel. The conclusion appears to be that all direct reactions are modified by dynamical nonlocality generated by couplings that are not specifically included in the calculation.

F. Further explorations

A full understanding of the nucleon-nucleus interaction is a very challenging formal problem. Some understanding might be possible within our general approach by interpreting the influence of changes in parameters. A single example of what might be possible is indicated in line L4X of Table I. In this case, halving the absorptive central term in the deuteron channel optical potential for L4 pickup led to the following changes:

(1) The magnitudes of both ΔJ_R and ΔJ_{IM} are substantially greater when the absorption in the deuteron channel is reduced.

(2) The smaller value of R_{CS} with reduced absorption in the deuteron channel reflects the much larger State CS value, 13.30 compared with 3.43. The smaller value of R reflects the somewhat larger ΔJ_{IM}. The increase in the CS value is not proportionate to the increase in State CS suggesting that the role of direct processes in leading to, or even suppressing, subsequent absorption, could be explored by such tests.

V. GENERAL CONCLUSIONS AND OUTLOOK

A. Pickup coupling for 40 MeV protons on ^{208}Pb

Coupling to pickup channels makes a very large contribution to the elastic scattering of 40 MeV protons on ^{208}Pb. The contribution of pickup coupling to the elastic channel proton-nucleus interaction has been reported before, Refs. [2,10–13], but is particularly large in this case, presenting an opportunity to study the mutual influences between different strongly populated pickup channels. The doubly closed shell property of ^{208}Pb also makes the contribution of inelastic scattering to low-lying collective states small, and these have been omitted from the present study. Previous studies suggest that the coupling effects investigated here would be larger at lower energies, and energy dependence will be the subject of future work. This has been studied for the case of protons on ^{40}Ca [13].

B. Nature of the DPPs

The contributions to the proton OMP revealed here cannot be represented by a smooth local additional potential, in particular not by a renormalization of a folding model potential. Although the effect of pickup is particularly large for proton scattering from ^{208}Pb it is a general effect for proton scattering. This is also true of coupling to inelastic channels, which happens to be small for ^{208}Pb, at least for low energy excitations. These various strong coupling effects suggest that the apparent success of the optical model for elastic scattering from nuclei may be deceptive. Arguably, coupled channel calculations for direct reactions of spectroscopic interest have cast doubt on conventional DWBA calculations. All couplings reflect back on the elastic channel and the appropriate elastic channel interaction is not in general the potential derived from folding models nor the potential that, on its own, fits elastic scattering data.

C. Coupling to multiple channels and dynamical nonlocality

The contribution to elastic scattering of neutron pickup is particularly strong for the ^{208}Pb target just as the contribution of inelastic coupling is small. The cases represented in Table I, arising from coupling to the states labeled L1 to L6, do not exhaust the possible important influences on elastic scattering of protons on ^{208}Pb. However, the six strongly coupled channels made it possible to study the interaction between channel couplings, in particular it is possible to explore how the DPPs for different couplings add when couplings are included together.

We discussed at some length how conclusions can be drawn concerning the dynamical nonlocality of the DPPs, a form of nonlocality quite distinct from the more familiar nonlocality arising from exchange processes.

The chosen pickup cases, L1 to L6, support a number of significant conclusions. When the DPPs are strong, as in cases L4 and L6, and even L3 for $r < 3$ fm, the DPPs do not add in the following sense. The local DPPs for coupling to state A or state B do not add to give the local DPP when both states A and B are coupled to the elastic channel. Thus the DPP for case L4L6, in which the elastic channel is coupled to both states L4 and L6, is not the sum of the DPPs for case L4 and case L6. This nonadditivity reflects the fact that the local equivalents of two nonlocal interactions do not add to give the local equivalent of the sum of the two nonlocal interactions; dynamical nonlocality is like exchange nonlocality in this respect. Thus the six couplings to states L1 to L6 individually are far from the total of couplings involving L1 to L6 that contribute to elastic scattering.

D. Concerning formal DPPs

We are not aware of any formal calculations of local and l-independent equivalents to the nonlocal and l-dependent theoretical DPPs. In practice, S-matrix inversion directly yields a local and l-independent representation of the DPP. There is also no available formal recipe for producing a local equivalent of the dynamical DPP, corresponding to the Perey factor for exchange nonlocality or its Perey-Buck representation. This would be difficult since the formal DPP is both nonlocal and l-dependent [4].

E. Influences between channels

An additional consequence of the dynamical nonlocality generated by coupling is the fact that channels that are not mutually coupled nevertheless influence each other when both are applied in a code such as FRESCO. It would seem that the origin of this property is related to the non-local effects discussed in Ref. [5]. This is a further reason why elastic scattering potentials should be adjusted to fit elastic scattering for each combination of coupled channels.

F. For future studies

State CS should be recorded in reaction calculations as a matter of course. Two matters of interest could be: (1) how does the State CS value, for a particular channel, vary as further channels, not coupled to the channel of interest, are introduced? (2) How are the changes in elastic channel cross section, when a state is coupled, related to the State CS? Here, and in earlier papers cited above, a range of properties have emerged; for example, the dependence on State CS is systematically dependent on whether the coupling is to rearrangement channels or inelastic channels, see, e.g., [2].

Future studies of nucleon-nucleus interactions with *ab initio* formalism and machine learning techniques will ultimately have to include pairs of nucleons in the continuum.

[1] G. R. Satchler, *Direct Nuclear Reactions* (Clarendon Press, Oxford, 1983).
[2] R. S. Mackintosh and N. Keeley, Phys. Rev. C **104**, 044616 (2021).
[3] H. Feshbach, Ann. Phys. **5**, 357 (1958); **19**, 287 (1962).
[4] G. H. Rawitscher, Nucl. Phys. A **475**, 519 (1987).
[5] N. Keeley and R. S. Mackintosh, Phys. Rev. C **90**, 044602 (2014).
[6] R. S. Mackintosh and A. M. Kobos, Phys. Lett. B **116**, 95 (1982).
[7] S. G. Cooper and R. S. Mackintosh, Inverse Probl. **5**, 707 (1989).
[8] V. I. Kukulin and R. S. Mackintosh, J. Phys. G: Nucl. Part. Phys. **30**, R1 (2004).
[9] R. S. Mackintosh, Scholarpedia **7**, 12032 (2012).
[10] R. S. Mackintosh and N. Keeley, Phys. Rev. C **85**, 064603 (2012).
[11] R. S. Mackintosh and N. Keeley, Phys. Rev. C **97**, 069901(E) (2018).
[12] N. Keeley and R. S. Mackintosh, Phys. Rev. C **97**, 014605 (2018).
[13] N. Keeley and R. S. Mackintosh, Phys. Rev. C **99**, 034614 (2019).
[14] R. S. Mackintosh and N. Keeley, Phys. Rev. C **100**, 064613 (2019).
[15] N. Keeley and R. S. Mackintosh, Phys. Rev. C **102**, 064611 (2020).
[16] R. S. Mackintosh and N. Keeley, Phys. Rev. C **98**, 024624 (2018).
[17] M. Matoba, K. Yamaguchi, K. Kurohmaru, O. Iwamoto, S. Widodo, A. Nohtomi, Y. Uozumi, T. Sakae, N. Koori, T. Maki, and M. Nakano, Phys. Rev. C **55**, 3152 (1997).
[18] I. J. Thompson, Comput. Phys. Rep. **7**, 167 (1988).
[19] W. W. Daehnick, J. D. Childs, and Z. Vrcelj, Phys. Rev. C **21**, 2253 (1980).
[20] R. V. Reid, Jr., Ann. Phys. (NY) **50**, 411 (1968).
[21] S. M. Smith, P. G. Roos, C. Moazed, and A. M. Bernstein, Nucl. Phys. A **173**, 32 (1971).
[22] R. L. Varner, W. J. Thompson, T. L. McAbee, E. J. Ludwig, and T. B. Clegg, Phys. Rep. **201**, 57 (1991).
[23] L. N. Blumberg, E. E. Gross, A. van der Woude, A. Zucker, and R. H. Bassel, Phys. Rev. **147**, 812 (1966).
[24] R. S. Mackintosh, Eur. Phys. J. A **55**, 147 (2019).
[25] N. Austern, Phys. Rev. **137**, B752 (1965).
[26] F. G. Perey and B. Buck, Nucl. Phys. **32**, 353 (1962).
[27] M. P. Fricke, E. E. Gross, R. J. Morton, and A. Zucker, Phys. Rev. **156**, 1207 (1967).